

Implementation of nonlinear control laws for an optical delay line ¹

John J. Hensch, Boris Lurie, Robert Grogan, Richard Johnson
Jet Propulsion Laboratory, California Institute of Technology
4800 Oak Grove Drive, Pasadena, CA 91109
818-354-2277
John.Hensch@jpl.nasa.gov

Abstract - This paper discusses the implementation of a globally stable nonlinear controller algorithm for the Real-time Interferometer Control System Testbed (RICST) brassboard optical delay line (ODL) developed for the Interferometry Technology Program at the Jet Propulsion Laboratory. The control methodology essentially employs loop shaping to implement linear control laws, while utilizing nonlinear elements as means of ameliorating the effects of actuator saturation in its coarse, main, and vernier stages. The linear controllers were implemented as high-order digital filters and were designed using Bode integral techniques to determine the loop shape. The nonlinear techniques encompass the areas of exact linearization, anti-windup control, nonlinear rate limiting and modal control. Details of the design procedure are given as well as data from the actual mechanism.

Keywords: Nonlinear control, coarse-vernier control, optical delay line, interferometer

TABLE OF CONTENTS

1. INTRODUCTION
2. LINEAR FEEDBACK COMPENSATOR DESIGN
3. NONLINEAR DYNAMIC COMPENSATION
4. ALGORITHM VALIDATION
5. CONCLUSION

1. INTRODUCTION

An optical interferometer is a device that creates an interference pattern from the light from small, spatially distributed collecting apertures in order to synthesize an image the resolution of a single large aperture telescope with a diameter equal to the separation distance of the two smaller telescopes. In so doing, it is able to perform various

astrometric measurements. The mechanism, which ensures that the light pathlengths from the two sources are adjusted properly in order to produce an interference pattern, is the optical delay line.

The brassboard ODL pictured in Figure 1 was designed to take a 3 cm diameter collimated beam of visible starlight and coaxial metrology beams and pass them on to a beam combiner. Light enters the bottom aperture and exits the top (or vice-versa). The ODL is composed of three tiered actuation stages to accommodate the large dynamic range requirement (1 m stroke with <5 nm stability). The coarse stage is a DC brushless motor with drive electronics that induce the motor to behave as a stepper motor. This motor moves a band that pulls a trolley on preloaded bearings at speeds up to 10 mm/sec. The main stage is a voice coil that actuates the main mirror, which is connected to the trolley by flexures. Finally, vernier stage is provided by a reactuated piezoelectric translator (PZT) mechanism beneath a 1.2 cm secondary mirror and operates over a range of 30 microns.

The control architecture may be viewed as in terms of a series of coarse-vernier loop structures. The fine control is done by the PZT. The function of the voice coil is to desaturate the PZT for commanded strokes larger than the saturation level of the PZT. The same coarse-vernier functionality exists between the voice coil and the motor stage.

The control system performance index is the root mean square error in the delay line pathlength. The principal design objective is to keep the root mean square error below five nanometers. Since disturbances typical for the ODL effect the pathlength error inversely proportional to the square of the frequency, it is necessary to design the control laws to reject these disturbances in proportion to their expected magnitude in the frequency domain.

In addition to the principal design objective, the following

¹ U.S. Government work not protected by U.S. copyright.

characteristics are required or highly desirable:

- system robustness with regard to both parametric uncertainties and nonlinear dynamics,
- good output responses to commands of different shapes and amplitudes,
- good transient responses to large amplitude vanishing disturbances that neither excessive large in amplitude nor duration, and
- Large disturbance/command triggering threshold of these nonlinear phenomena, in order that these nonlinear phenomena happen infrequently.

2. LINEAR FEEDBACK COMPENSATOR DESIGN

The main challenge in the design and implementation of the RICST optical delay line controller has been the design of the coarse-vernier loop for the PZT and the voice coil systems. The linear design approach extends the work of Lurie, et al [9]. The modeling of the physical plant, that is, the systems actuated by the PZT, Voice Coil, and Motor is based on the work of Grogan et al. [3]. Details of the mechanical, electronic, and software design may be found in [2], [4], and [5] respectively. To aid the discussion of the linear compensator design, a block diagram of the control design with the nonlinear elements removed is depicted in

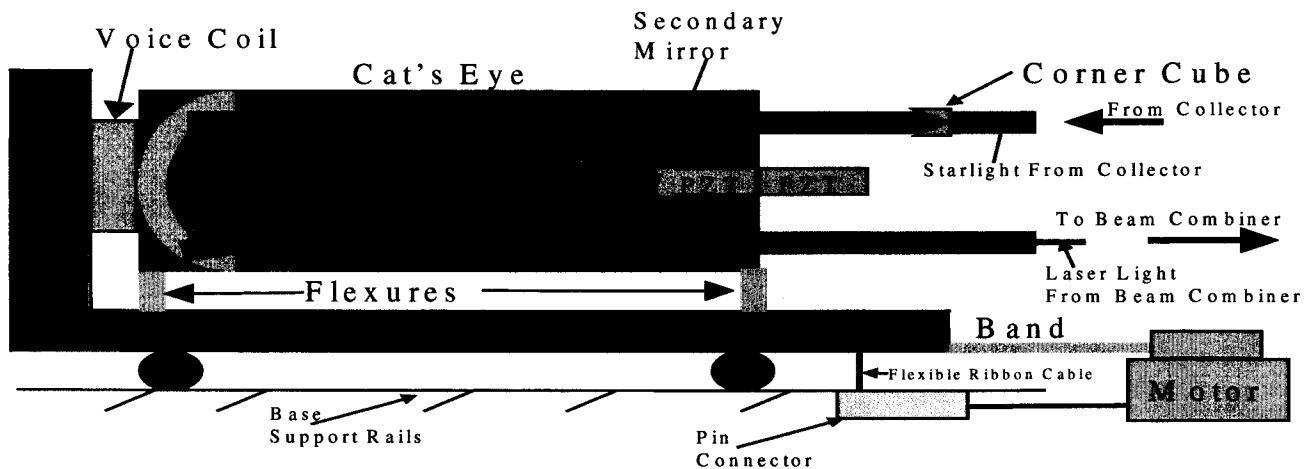


Figure 1 Optical Delay Line Diagram

One important feature of the Real-time Interferometer Control System Testbed (RICST) optical delay line is that for all of its stages Coulomb friction plays a minimal role in the dynamics of the system. As a result, the system behaves very linearly for displacements of the actuators within its actuation range. This fact permits the following design philosophy:

1. Implement the basic design of the control algorithm as a linear compensator. Use a Bode-integral approach to the controller design to yield a high-order controller providing robust stability especially to non-linear phenomena which have their effects above the bandwidth of the controller [1].
2. Use nonlinear dynamic compensation to ensure that the loops remain stable even for transients or commands that saturate the actuators, since actuator saturation is the dominant nonlinear component of the plant [6,8].
3. Validate the control algorithm using a detailed simulation of the system.

Figure 2 and is described in detail below.

- The PZT plant is modeled as the following dynamic systems connected in series:
 - A second order mechanical system with the underdamped resonance at 3800 Hz
 - An LC circuit with time constant of 0.28 ms which is associated with its drive electronics,
 - A zero-order hold with sample rate of 5000 Hz,
 - A pure time delay of 0.1 ms associated with computing the control laws and outputting the results. The Bode diagram of the transfer function of these elements connected in series is depicted in Figure 4.
- PZT open loop bandwidth is 325 Hz wide, with a Bode step response, with the slope -10 dB/octave at frequencies 10 to 650 Hz, rolling off at lower frequencies, as depicted in Figure 5. This provides 30 degrees of phase margin below 650 Hz and 10 dB of gain margin above 650 Hz, as shown in Figure 6. The phase margin of 30 degrees was maintained for open-loop amplitudes between 0 and -10 dB to ensure, among other things, good robustness to nonlinear

effects such as current limiting in the high voltage PZT driver or the hysteresis of the PZT stack.

- The voice coil plant is modeled as the following dynamic systems connected in series:
 - A second order mechanical system with the underdamped resonance at 3.8 Hz
 - An LC circuit with time constant of 0.35 ms which is associated with its drive electronics,
 - A zero-order hold with sample rate of 2500 Hz,
 - A pure time delay of 0.1 ms associated with computing and outputting the control laws. The Bode diagram of the transfer function of these elements connected in series is depicted in Figure 6.
- The voice coil loop is designed to operate in parallel with the PZT loop. To ensure that the total transfer function of these parallel loops remain minimum phase, the phase difference between the loops is less than 180 degrees. (This is a sufficient condition for minimum

phase of a filter comprised of two minimum phase filters connected in parallel [7]). The voice coil loop is designed such that the gain of the voice coil loop is greater than the gain of the PZT loop below 55 Hz, and is depicted in Figure 8.

- The motor plant is modeled simply as a velocity-drive motor, *i.e.*, the transfer function from command to position is simply a single integrator times a constant.
- The motor loop is designed to zero the voice-coil offset. It estimates the voice-coil offset using low-pass and sinc (moving average) filters in series, and then uses a proportional gain constant to scale the offset for the feedback command. The motor loop also incorporates a feedforward command pass that estimates the desired velocity from the input command and feeds this forward to the motor command. The feedforward pass also includes sinc filters as not to excited the 3.8 Hz mode of the cat's eye structure.
- To minimize the effect of command disturbance

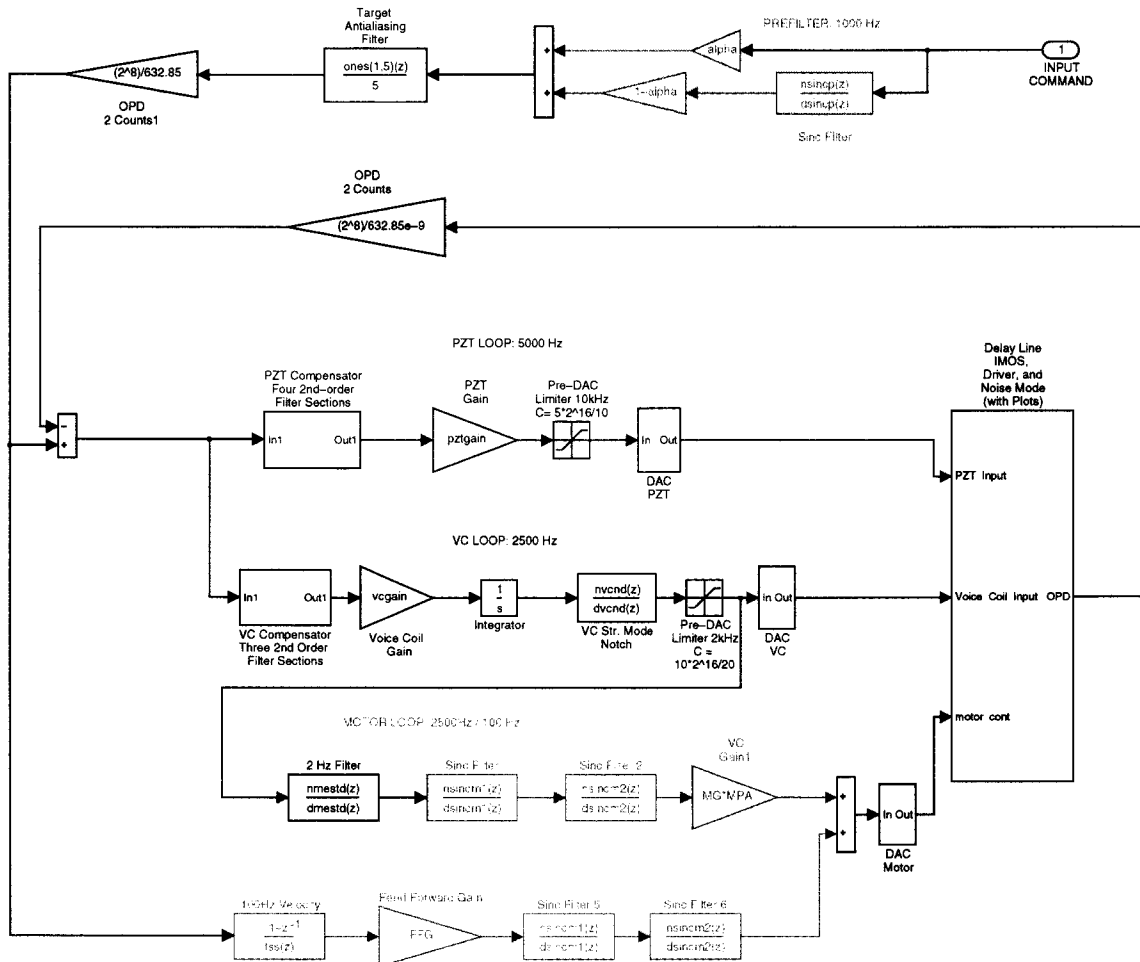


Figure 2 Controller Block Diagram with only Linear Elements Shown.

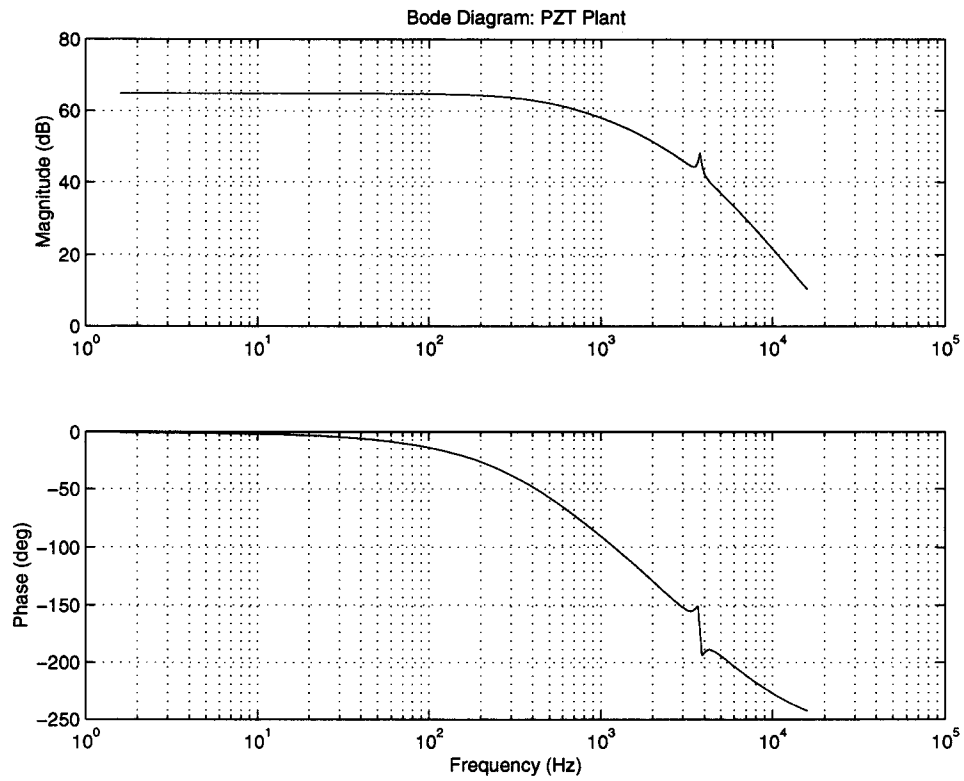


Figure 3 Bode Diagram of the PZT plant

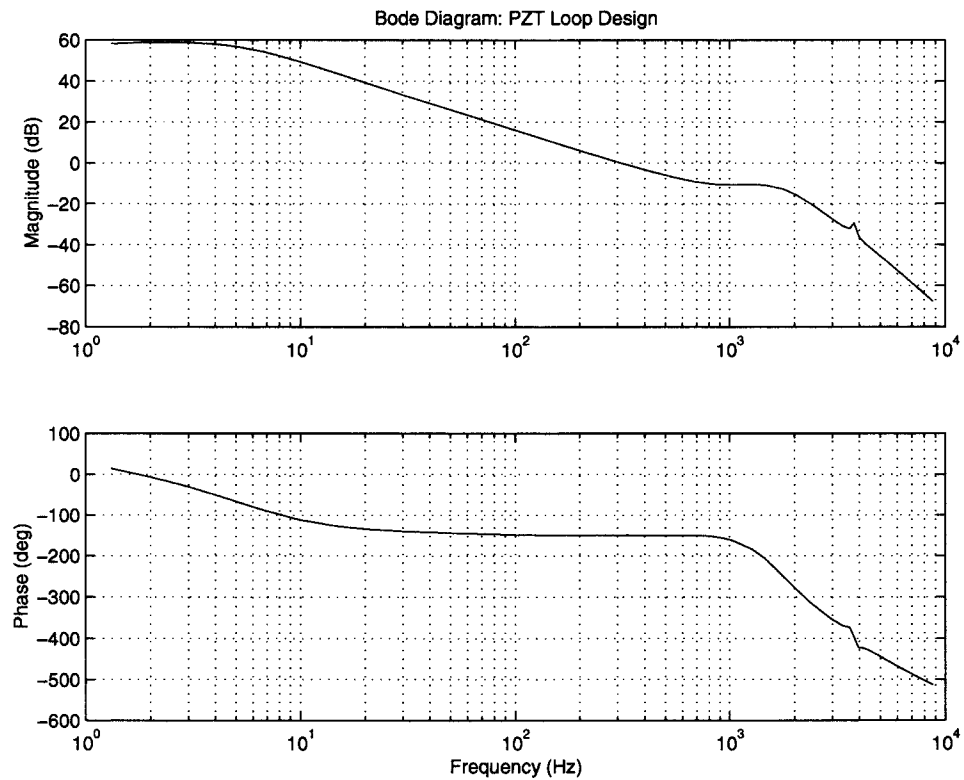


Figure 4 Bode diagram of the PZT open loop transfer function

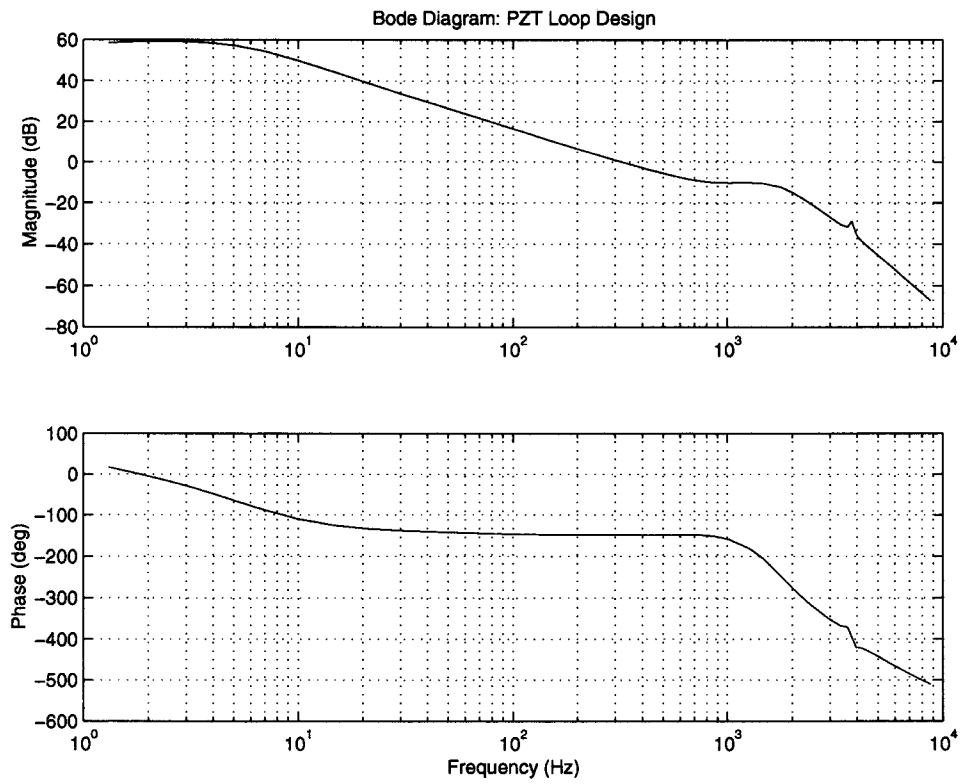


Figure 5 Bode plot of the PZT open loop transfer function

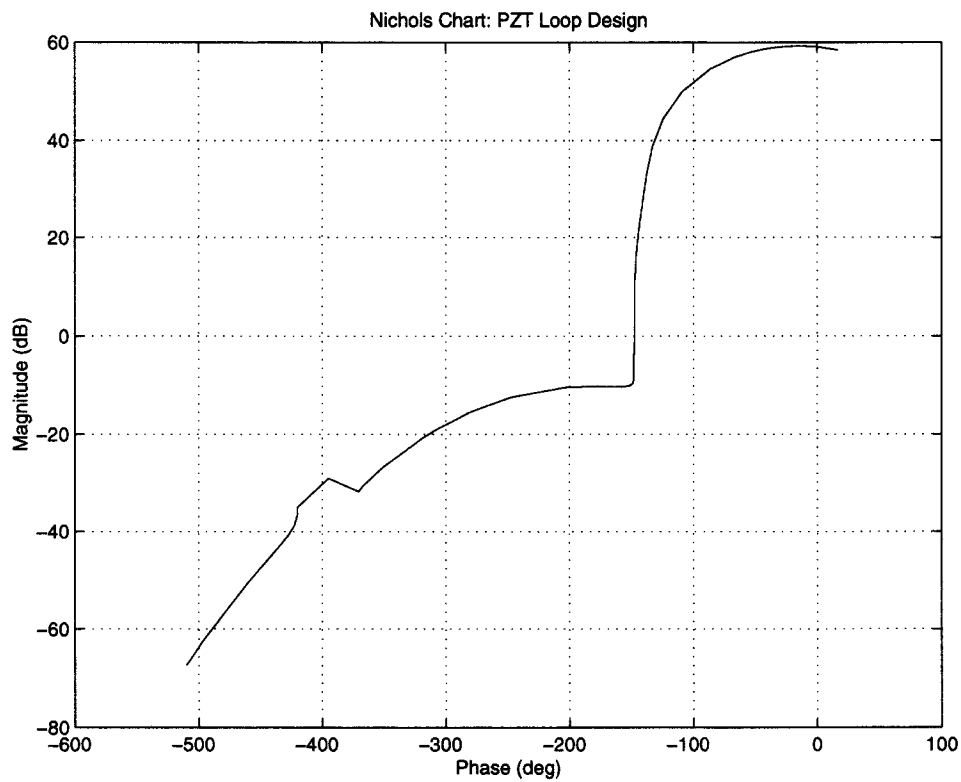


Figure 6 Nichols Chart of the PZT open loop transfer function

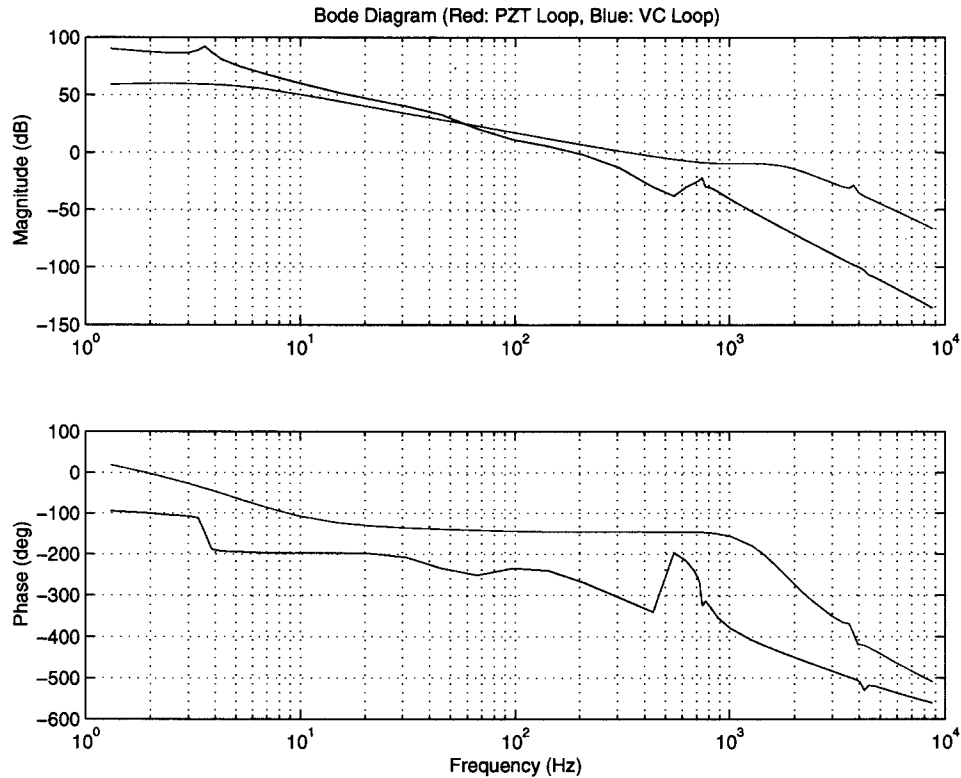


Figure 7 Bode plot of the voice coil and PZT open loop transfer functions

amplification of those frequencies near the bandwidth of the controller a command prefilter is added to the input pass. This design uses a sinc (moving average) filter whose first notch is tuned to the open-loop crossover frequency of the feedback loop. The depth of the notch is adjusted by varying the relative weighting of the filtered pass to a unity pass in a parallel structure. To minimize size of the sinc filter, the sinc filter is operated at 1000 Hz instead of 5000 Hz. A separate anti-aliasing filter is added to smooth the output of the 1000 Hz filter.

The PZT and voice coil controllers were designed by iterative methods as high order continuous time filters. Once the proper loop shape was attained the continuous time controllers were factored into second order filter sections and converted to second-order discrete-time filters by a continuous to discrete transformation with prewarping about the dominant frequency of the second-order section. The resultant PZT and voice coil compensators comprised four second order sections each.

3. NONLINEAR DYNAMIC COMPENSATION

To meet the secondary design objective of good transient response to large amplitude disturbances, the linear loops described above are augmented with nonlinear dynamic compensation. This design objective is in fact quite important, because these types of transients are often encountered during system initialization. Furthermore, robustness to large actuator saturating transients allows for modal or switching control, where different controllers are swapped in and out depending on the magnitude of derivative of the input command or of the control error. For the RICST optical delay line controller, the nonlinear dynamic compensation may be grouped into four categories: exact linearization, anti-windup control, non-linear rate limiting control, and modal switching control.

Hierarchically, the first instance of nonlinear dynamic compensation addresses the saturation in the PZT actuator. This saturation is due to the digital to analog converter, which only allows, via the high voltage PZT driver, a range of only 100 volts to be outputted to the PZT actuator. Since the voice coil loop alone is unstable and must be stabilized by the PZT, any transient which forces the PZT into saturation can possibly destabilize the whole loop unrecoverably. The fact is attested to both in simulations and

the voice coil loop alone is unstable and must be stabilized by the PZT, any transient which forces the PZT into saturation can possibly destabilize the whole loop unrecoverably. The fact is attested to both in simulations and in practice.

The solution to this problem is to create an additional loop about the PZT plant, which in effect removes the saturation nonlinearity. This is accomplished by first placing a dead-zone in parallel with the saturation due to the digital to analog converter, as shown in Figure 8. Note that if the width of the dead zone exactly equals the nonsaturating range of the saturator, then the sum of signals b and c is the signal a . If a digital filter (PZT pseudo-plant) is then designed such that it has the same transfer function as the PZT plant, the sum of signals f and g are equivalent to the signal a passing through a linear plant without the saturation nonlinearity. This linearization prevents the voice coil loop from going unstable because the input to the voice coil is not the actual OPD error, but the OPD error "linearized" by the PZT pseudo-plant. It should be noted that the term "exact

the voice coil compensator's integrator state due to limited actuation of the voice coil. This windup produces poor transient behavior to large disturbances. This problem is eliminated by separating the integrator state from the compensator and replacing the integrator by a limited integrator. Simulations indicate that a factor of three separation between the maximum amplitude of the limited integrator and the rails of the saturator is sufficient for stability; however, a factor of 10 was maintained in the implemented hardware. This is depicted in Figure 9.

The third instance of nonlinear dynamic compensation deals with the fact that the rates in the motor stage should be limited to a maximum value. Rate saturation is a phenomenon that appears most often when the delay line motor is commanded to slew rapidly between to positions. The controller uses a switching type controller to command these large slews. The controller switching is decided by measuring the controller error. When the controller error reaches the slewing threshold, the error inputs to the voice coil and PZT paths are set to zero, and the motor velocity

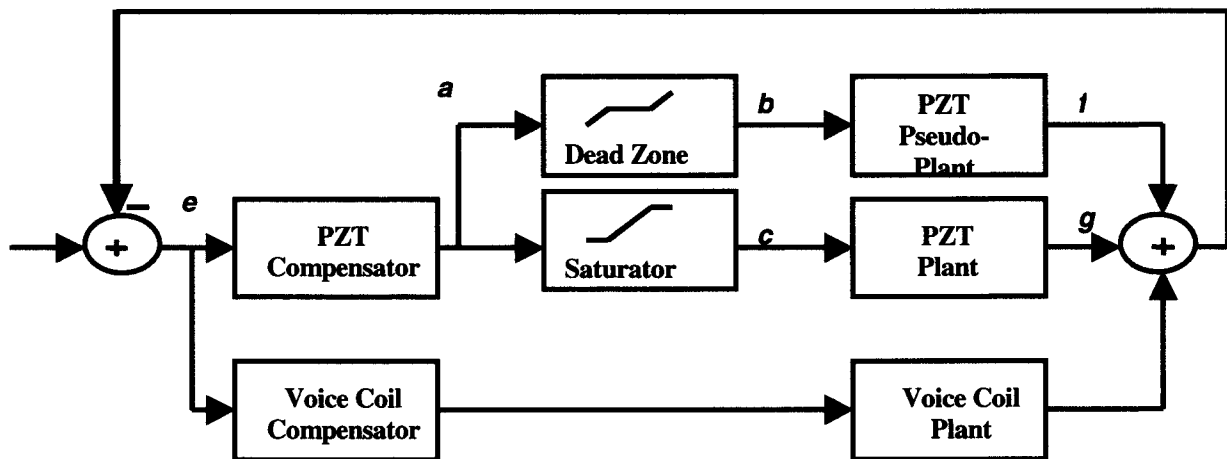


Figure 8 Exact Linearization of the PZT plant

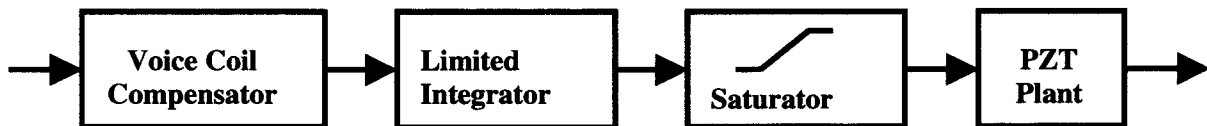


Figure 9 Antiwindup control for the Voice Coil loop

linearization" may in fact be misleading: it has been shown in simulation that this linearization quite robust with regard to mismatches between the dead zone and the saturator, and between the PZT plant and PZT pseudo-plant.

The next instance of nonlinear dynamic compensation addresses the saturation of the voice coil actuator. Again, this saturation is due to the digital to analog converter in the voice coil path. The main problem in this case is wind up of

command V_{mc} is given by (1), where x_{stop} is the stopping distance, e is the controller error, V_{max} is the maximum desired carriage velocity and V_{min} is the minimum desired carriage velocity.

Once this controller moves the delay line to a position where the PZT and voice coil can track the input command, that is, when the controller error is less than a tracking threshold, the nonlinear compensation is no longer active and the

motor controller reverts to a linear controller. The tracking and slewing thresholds are set with a hysteresis of approximately a factor of 10 for stability, about 100 μm for the tracking threshold, and 1 mm for the slewing threshold.

The nonlinear motor slewing controller uses a sinusoidal profile because it introduces little to no jerk into the delay line. In fact, when the V_{\min} is zero, the solution of the differential equation arising from the control law may be written in closed form. This may be seen by noting that $\dot{x} = -V_{\max} \sin^2 x$; $x(0) \in [0, \pi/2]$ has as its solution $x(t) = V_{\max} \cot t$. The velocity profiles produced by the control motor control law behaves similarly to the closed-form solution and does indeed allow for the transition from a constant velocity to a stop in a smooth fashion.

A block diagram of the control design with the nonlinear elements included is depicted in Figure 10.

$$V_{mc} = \begin{cases} -\operatorname{sgn}(e) \left(\frac{V_{\max} + V_{\min}}{2} - \frac{V_{\max} - V_{\min}}{2} \cos\left(\frac{\pi |e|}{x_{\text{stop}}}\right) \right); & |e| < x_{\text{stop}} \\ -\operatorname{sgn}(e) V_{\max}; & |e| > x_{\text{stop}} \end{cases} \quad (1)$$

4. ALGORITHM VALIDATION

The validation of the RICST optical delay line controller comprised two methods: frequency and time domain. Frequency domain methods were used to measure the open-loop transfer function of the PZT and voice coil loops. These were then compared with the designed loops. Also, the closed loop transfer function of the PZT and voice coil loops operating in parallel was measured. These measurements were taken using a DSPT Siglab virtual network analyzer (VNA). To measure the open-loop transfer functions of the PZT, persistent excitation provided by the VNA was applied to the inputs to the PZT controllers (point e in Figure 9). The optical pathlength variation was measured by the VNA and the transfer function was computed. The input signals were kept small enough that the PZT plant did not go into saturation. Also, while the measurements were taken, the signal path through the voice coil was disabled by switching off the power to the voice coil amplifier. A similar measurement was taken, but this time the signal path was routed not through the PZT plant, but through the PZT pseudo-plant alone. Finally, a similar procedure for measuring the open-loop transfer function of the PZT loop was repeated for the voice coil loop. The only difference was that the voice coil compensator was modified below 4 Hz; a high-pass filter was added such that the integrator roll-off below 4 Hz was replaced with a constant

gain below 4 Hz. This prevented the open-loop plant from going into saturation for some small input bias. Without this modification, the VNA would not have been able to take meaningful measurements.

The results of the open-loop transfer function measurements are depicted in Figure 11. Note that the transfer function for the PZT plant (blue) and the PZT pseudo-plant (green) agrees quite well with the designed loop (red). Note too that the designed (black) and measured (magenta) voice coil transfer functions are nearly the same for frequencies below 200 Hz; the measurements above 200 Hz were dominated by noise.

Once the open-loop transfer functions were taken the PZT and voice coil loops were closed and the closed-loop transfer function of these loops operating in parallel was measured. The measurement was taken twice, once with the prefilter section removed, and once with the prefilter section included. The results of the closed-loop transfer function

measurements are depicted in Figure 12. Note the smooth roll-off characteristics of the closed-loop system with the prefilter added.

Frequency domain techniques were also used to measure the amount of closed loop disturbance rejection. The testbed was outfitted with dynamic shakers that introduced a disturbance force to the optical table. The spectra of the disturbance force was determined by the input to the shaker amplifier, which was wideband (5000 Hz) white noise. Data was taken for 40 seconds; the loop was open for the first 18 seconds, then closed for 15 seconds then opened again. Figure 13 shows the time history of the experiment. Note the reduction of the error while the loops were closed from 18 to 33 seconds in the time history. Next, a power spectral density was estimated using the open and closed loop data. Ten separate one second data samples were averaged to make the PSD, which is depicted in Figure 14.

Time domain methods were used to measure the response of the closed-loop transfer function to a number of inputs and/or disturbances, and to test for global stability. Figure 15 shows the response to a small step amplitude change in the delay line command (about 1250 nm of OPD). For such a command, the actuators operate within their linear range. The rise time of 1.5 ms is consistent with the 325 Hz bandwidth controller. Figure 16 shows the response to a large small step amplitude change in the delay line command (about 31,000 nm of OPD). The step response is markedly different, but nonetheless stable. For such a large step, the controller goes into five separate regimes:

1. PZT and voice coil active
2. PZT saturated and voice coil active and slewing,
3. PZT and voice coil saturated,
4. Voice coil saturated and PZT active,
5. PZT saturated and voice coil in limit cycle.

The behavior of the optical delay line is different in all of these regimes, and is depicted in detail in Figure 17. In the upper left-hand plot, the transition from the linear regime to nonlinear regime is noted. At first the OPD rate is quite fast, but as soon as the PZT saturates, the OPD rate is reduced. In the upper right-hand plot, both the PZT and the voice coil actuators are in saturation. As a result, the structural mode of the cat's eye is excited, but not damped by the controller, which causes the sinusoidal dip in the plot. In the lower left-hand plot, the voice coil actuator is still in saturation, but the sign of the error flips as the OPD moves past the commanded OPD. The PZT then goes out of saturation and tries to stabilize the plant at about 2.88 seconds on the plot. At about 2.9 seconds, the overshoot of the OPD is too large for the PZT and it goes back into saturation. This same phenomenon is repeated at about 3.1-3.2 seconds and after 3.4 seconds on the plot (see Figure 16). In the lower right-hand plot, the PZT is in saturation and the voice coil is active and in a limit cycle with characteristic frequency of 85 Hz. The dynamics of the limit cycle was analyzed in detail in [9]. In computer simulations, the limit cycle was induced by eliminating the PZT plant, but retaining the PZT pseudo-plant. This produced a similar limit cycle with approximately the same characteristic frequency.

Finally, Figure 18 shows the global stability characteristic of this implementation of the RICST optical delay line controller. The delay line is in tracking mode and is manually moved. The amplitude of the disturbance is 1.5 mm, which is five orders of magnitude above the steady state tracking error. The dominant mode of the disturbance is the mechanical resonance of the cat's eye. This mode is quickly damped and the delay line returns to tracking mode. For disturbances as large as this, the modal switching of the delay line control is exercised, and shown to exhibit good stability properties.

5. CONCLUSION

The control system for the RICST optical delay line is a complex algorithm which enables it to track a OPD command with small error while being able to maintain stability over the entire operating range of the instrument. The design philosophy has embraced two areas of controller design which are not commonly used in practice. The first is the use of Bode integral laws to formulate the loop shape.

Since the loop shape is determined by these integrals and not by limiting the order of the controller *a priori*, the controller that achieves this loop shape is necessarily of high order. The validation of the loop shapes by simulation and measurement indicates that such a high-order controller may be used without numerical or computational difficulties.

The second design philosophy was the liberal use of nonlinear controllers. This is especially important for this application which has by necessity a coarse-vernier feedback architecture. This has increased the performance of the optical delay line with regard to these important aspects:

- It provides stability over all possible operating ranges
- It provides smooth transients to disturbances overloading the vernier actuator.
- It provides good transient response to the command, with negligible overshoot and small rise- and settling-times
- It allows simplifying the commander by commanding only the destination point, *i.e.*, using a step-function command and not a time-profiled command

ACKNOWLEDGEMENT

This research was carried out by the Jet Propulsion Laboratory, California Institute of Technology, under a contract with the National Aeronautic and Space Administration.

REFERENCES

- [1] H. W. Bode, *Network Analysis and Feedback Amplifiers design*. Van Nostrand, New York, 1945.
- [2] R.J. Calvet, B. Joffe, D. Moore, R.L. Grogan, and G.H. Blackwood, *Enabling Design Concepts for a Flight-Qualifiable Optical Delay Line*, Proceedings of the 1998 SPIE Astronomical Interferometry Conference, Vol. 3350-64.
- [3] R. L. Grogan, G. H., Blackwood, and R. J., Calvet, *Optical Delay Line Nanometer Level Pathlength Control Law Design For Space-Based Interferometry*, Proceedings of the 1998 SPIE International Symposium on Astronomical Telescopes and Instrumentation Astronomical Interferometry, April 1998.
- [4] P. Irwin and R. Goullioud, *Hardware Design and Object-Oriented Hardware Driver Design For The Real Time Interferometer Control Systems Testbed*, Proceedings

of the 1998 SPIE Astronomical Interferometry Conference,
Vol. 3350-76.

[5] R. Johnson, E. McKenney, D. Slye, and K. Starr, *Real Time Control Software For Optical Interferometers: The RICST Testbed*, Proceedings of the 1998 SPIE Astronomical Interferometry Conference, Vol. 3350-77.

[6] B. J. Lurie, *Feedback Maximization*. Artech House, Dedham, MA, 1986.

[7] B. J. Lurie. On Zeros of the Sum of Two Impedances in the Right Hand Half Plane. "Telecommunications", no. 9, 1962.

[8] B. J. Lurie and P. J. Enright, *Classical Feedback Control with MATLAB*, Marcel Dekker, New York 2000.

[9] B. J. Lurie, J. J. Hench, A. Ahmed, and F. Y. Hadaegh, *Nonlinear control of the optical delay line pathlength*, Proc. of the SPIE conference, April 1999, V. 3692, pp. 139-149.

John Hench received his B.S. from U.C. Berkeley in 1983 and his M.S. and Ph.D. from UCSB in 1989 and 1992 respectively. He has worked as a Fulbright Fellow at the Institute of Information Theory and Automation of the Czech Academy of Sciences and as a Royal Society Fellow at the University of Reading, England. Presently, he is a member of the Guidance and Control Analysis Group at the Jet Propulsion Laboratory in Pasadena, California. His research has been in the areas of optimal control, numerical analysis, estimation, and nonlinear control.

Boris J. Lurie is a member of technical staff in the Guidance and Control Analysis Group at the Jet Propulsion Laboratory since 1986. He has degrees of M.E.E. in Telecommunications from the Institute of Telecommunications, St.-Petersburg, Ph. D. from the Institute of Transportation, St.-Petersburg, and Dr. of Eng. Sciences from VAC, Moscow, Russia. His research has been in the areas of network synthesis, feedback amplifiers, and nonlinear oscillation and control. He holds 9 patents, and his publications include 6 books. Dr. Lurie worked in Russian Telecommunication Research, Israel Ministry of Telecommunication, TRW, and JPL, consulted for industry, and taught at universities in Russia, Israel, and USA. He is a member of AIAA.

Robert L. Grogan is a Senior Member of the Technical Staff at the Jet Propulsion Laboratory. He works on the Space Interferometry Mission and is responsible for the technical leadership of a multidisciplinary team which integrates the optics, structures, and control disciplines into computational dynamics models of the mission flight system. He was previously a Staff Engineer at AlliedSignal Aerospace Guidance and Control Systems. He received a B.S. degree from The Pennsylvania State University in 1992 and a M.S. degree from the Virginia Polytechnic Institute and State University in 1994.

Richard Johnson is the principal software architect of the Real-time Interferometer Control Systems Testbed (RICST) at JPL. He has a BS EE and MEng EE from Cornell University.

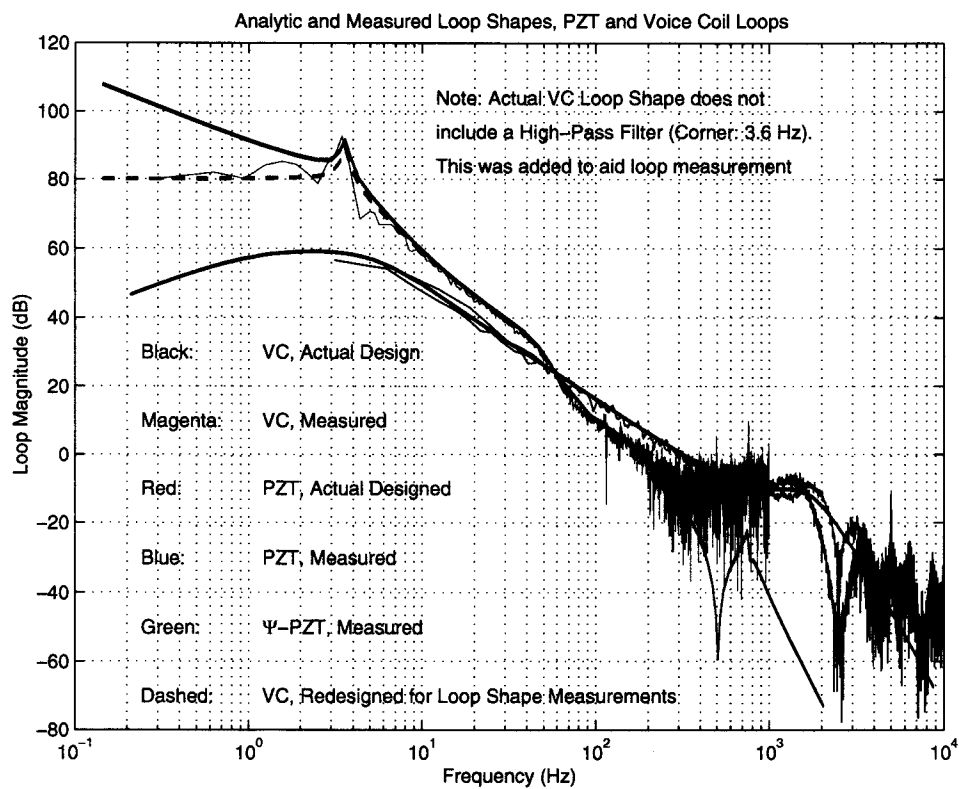


Figure 11 Measured Open Loop Transfer Functions

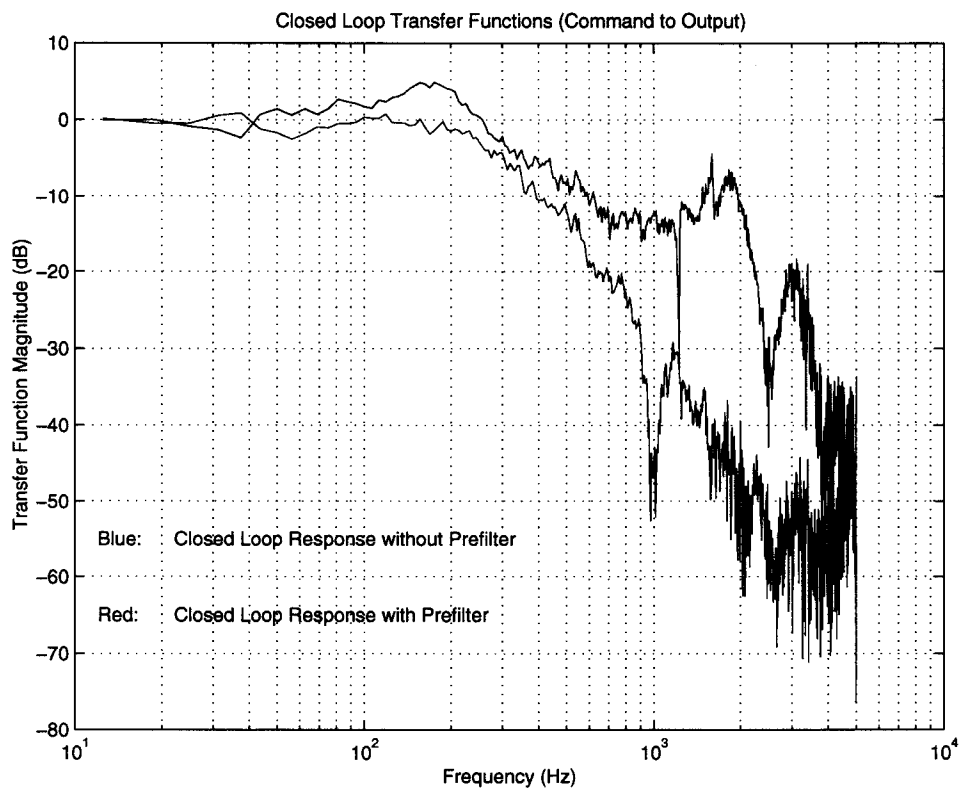


Figure 12 Closed Loop Transfer Functions

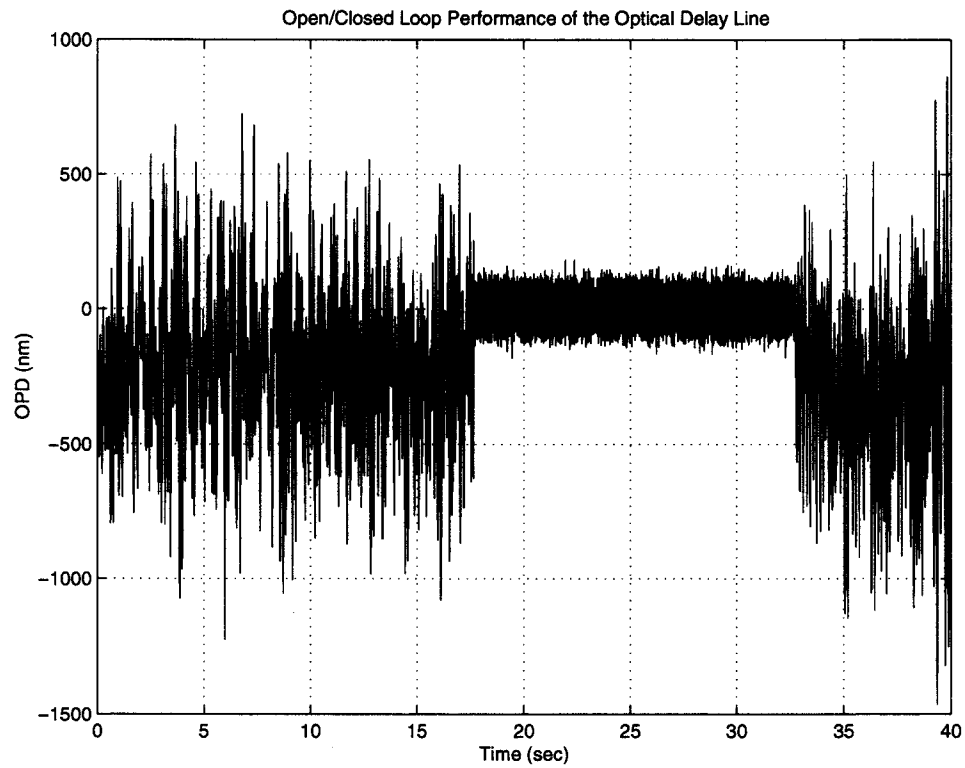


Figure 13 Time History Open/Closed Loop Performance

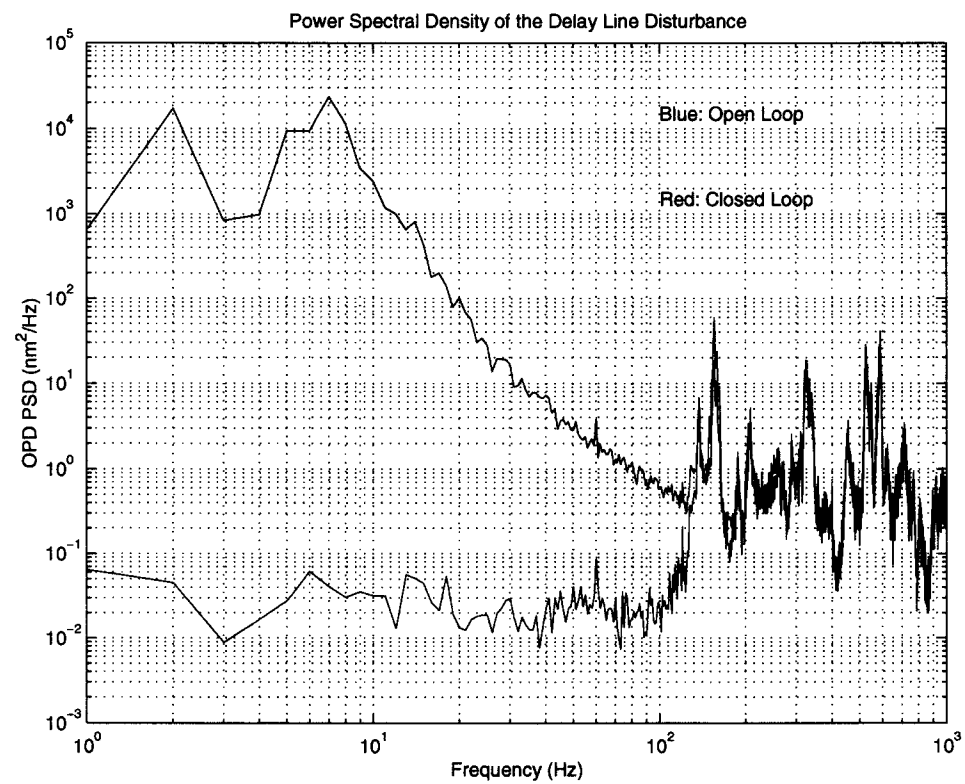


Figure 14 Open/Closed Loop Disturbance PSD

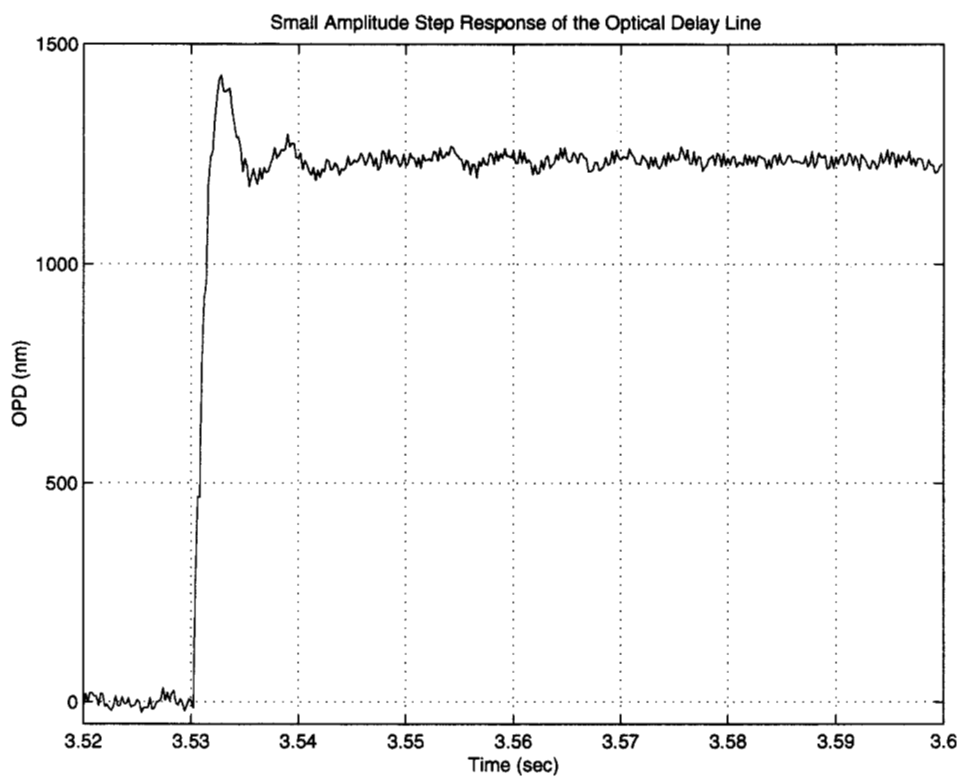


Figure 15 Step Response

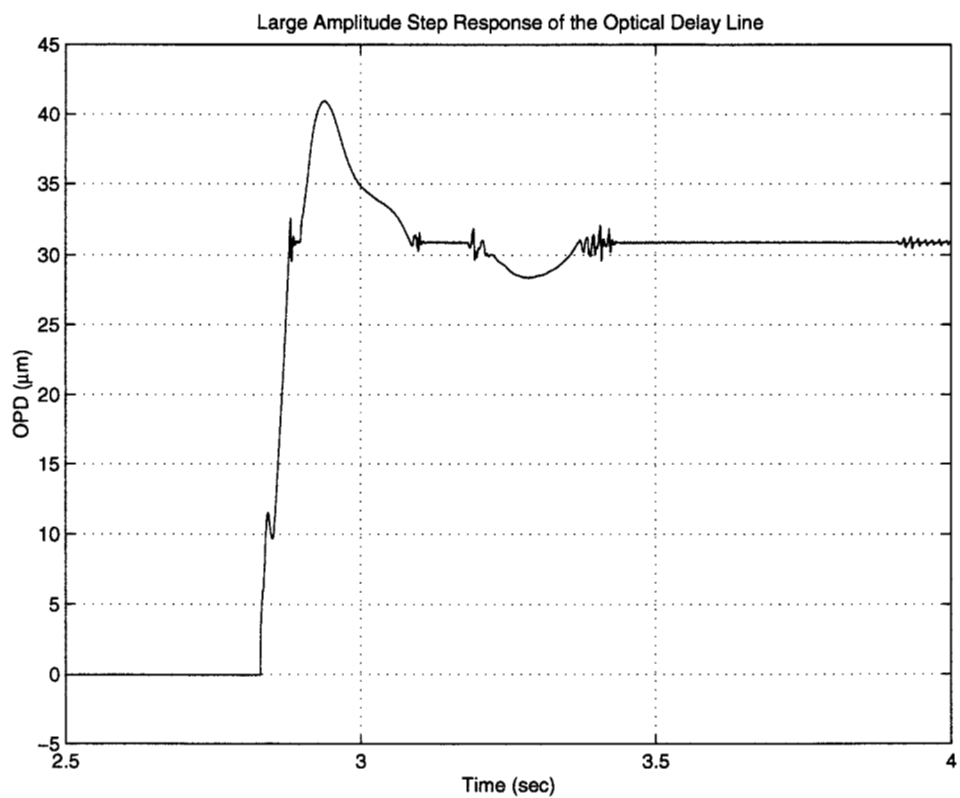


Figure 16 Large Amplitude Step Response

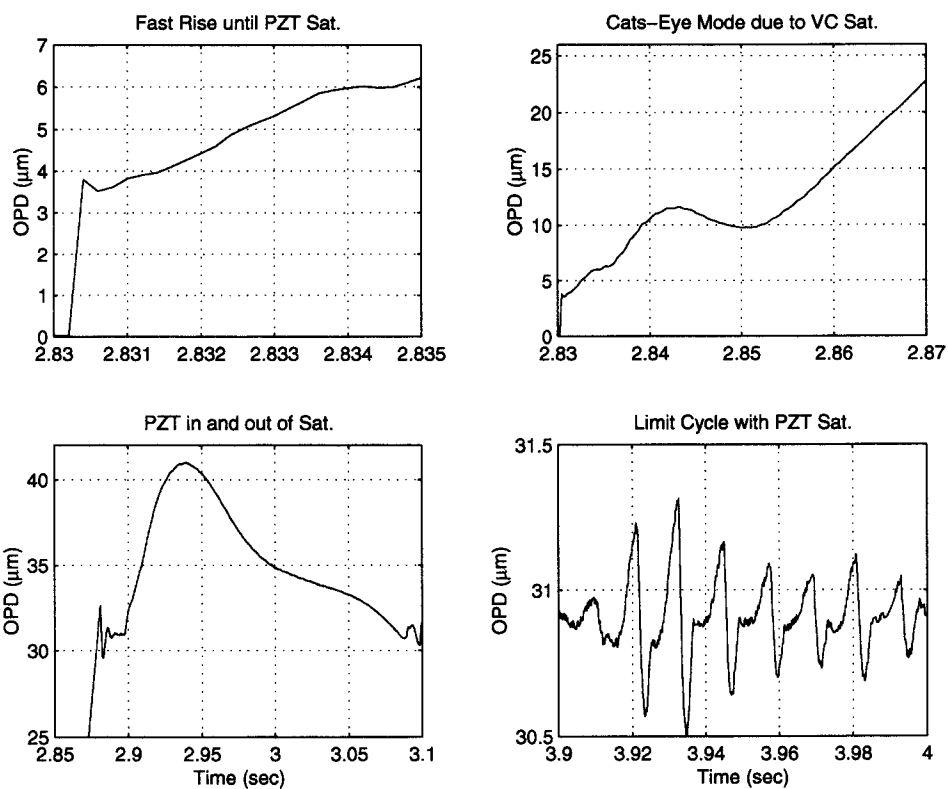


Figure 17 Large Amplitude Step Response (Detail)

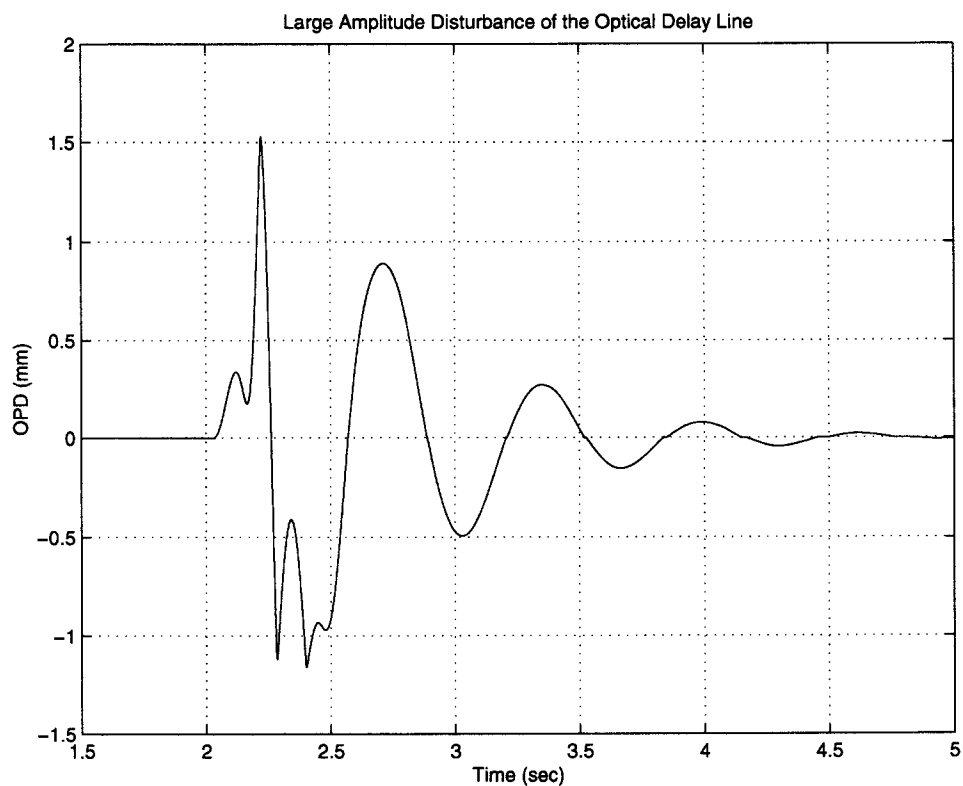


Figure 18 Large Disturbance Response